Coupled vesicle morphogenesis and domain organization

Changjin Huang, Hongyan Yuan, and Sulin Zhang[a)]
Department of Engineering Science and Mechanics, Pennsylvania State University, Pennsylvania 16802, USA

(Received 13 August 2010; accepted 10 January 2011; published online 26 January 2011)

Protein-enriched membrane domains with distinct biophysical properties have been thought as the basic organizing units of cellular membrane. Using particle dynamics simulations, here we study phase separation dynamics and domain formation in binary vesicles. Our simulations clearly show the intimate coupling between domain compositions, lateral domain organization, and vesicle shape transformation. Our simulation results provide insights into the essential role of membrane domains in the coordinated remodeling of cellular membranes and in protein and lipid sorting. © *2011 American Institute of Physics*. [doi:10.1063/1.3549176]

Much attention has been paid to the formation mechanism of lipid rafts that arise from segregation of lipid phases.[1] Yet, the concept of membrane domains has recently gone beyond the classical lipid rafts. It is now generally accepted that molecular interactions lead to segregation of proteins and lipid components, forming small submicron membrane domains of distinct compositions. The protein-enriched membrane domains are thought to be the basic organizing units of cell membranes and serve as platforms for biomedical signaling,[2,3] trafficking,[4] and material transport.[5–7] On the microscale, the two-dimensional character of cellular membranes allows bending into three-dimensional shapes under physiological conditions, creating diverse long-range membrane morphologies. Membrane domains constituted of scaffolding proteins or transmembrane proteins of specific shapes can locally modify membrane curvatures, perturbing or even causing long-range remodeling of membrane morphology.[8–12] Reciprocally, the long-range membrane morphology imposes an elastic field onto membrane domains, modulating domain growth dynamics and tempospatial domain organization.[13–16] Despite extensive research on the lipid rafts in the past decade, experiments remain rare in characterizing the coupling between the long-range membrane morphogenesis and the short-range domain compositional and spatial organization.[17,18]

In this letter, we elucidate the coordinated interplay between the shape transformation of a binary vesicle and the phase separation and subsequent domain organization based on a recently developed particle-based membrane model.[19] Through simulations, we wish to provide insights into the regulatory mechanisms of the size and spatial localization of membrane domains, and shed lights on membrane domain mediated protein and lipid sorting. The particle-based membrane model features a soft-core interparticle potential with the interaction energy well depth ϵ weighed by the relative orientations of the particle pair. The model is solvent-free, where the hydrophobic interaction is reinstated through the orientation-dependent interparticle potential. The model introduced three model parameters, μ, ς, and θ_0, which independently tune, respectively, the bending rigidity, diffusivity, and spontaneous curvature of the simulated membrane. The length and time scales of the particle-based model are on the order of $\sigma \sim 1.4$ nm and $\tau \sim 0.1$ μs, respectively, which represents a higher level of coarse-graining than the chain-of-bead models.[20–25] The particle-based model reproduces a wide range of experimentally observed equilibrium configurations of homogeneous vesicles and provides additional aspects regarding the dynamic morphological evolution of vesicles.[26]

Here, we extend the particle-based model to study phase separation dynamics in a binary vesicle. In the experiments, the volume of fluid vesicles can be regulated by controlling the osmotic pressure difference across the membrane, which can be realized by tuning ion concentration in the solution. On the other hand, temperature quenching initiates phase separation.[27] These two events may occur simultaneously or sequentially with specified order. To induce the whole-vesicle shape transformation, we control the volume of a binary vesicle by adding a global external potential $E_V = \frac{1}{2}k_V(V/V_0-1)^2$, where V_0 and k_V are the desired volume and the volume spring constant, respectively. The instantaneous volume V of the vesicle is calculated via a local triangulation mechanism.[26] Domain separation dynamics in a binary vesicle has been previously studied via a similar method.[28] However, global shape transformation was not implemented; the properties of the simulated lipid membrane are yet to be reported.[29] We represent the binary vesicle as a particle assembly with two different particle types, the primary particle type A and the secondary particle type B, differentiated by assigning different model parameters. We assign $\epsilon_{AA}=\epsilon_{BB}=1.0\epsilon$ and $\epsilon_{AB}=0.7\epsilon$. The different interaction strengths give rise to the line tension of the two phases $\sim\lambda = 4.4\times10^{-12}$ N, which falls in the range of the experimental data.[30] Considering the stiffening role of the proteins and the lipid rafts,[13,31] we set $\mu_{AA}=3.0$, and $\mu_{AB}=\mu_{BB}=6.0$, corresponding to bending rigidities of $25k_BT$ and $53k_BT$, respectively, with k_BT being the thermal energy. We assume a zero spontaneous curvature ($\theta_0=0°$) for the primary phase, while allow that of the secondary phase to vary. We set $\varsigma=4$, yielding the diffusion constant $D=0.06\sigma^2/\tau$. All the simulations performed here are in the *NVT* ensemble, with a total of 11 054 particles and at $k_BT=0.2\epsilon$.

Figure 1 shows the shape transformation pathways of the binary vesicle with a low compositional ratio (B:A = 1:9). The simulations start from a spherical vesicle with randomly distributed phase particles. All the shapes are

a)Electronic mail: suz10@psu.edu.

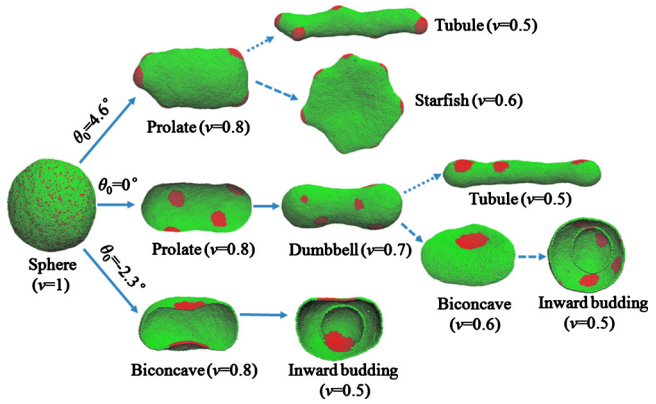

FIG. 1. (Color online) Shape transformation pathways of binary vesicles with a low compositional ratio (B:A=1:9). Three pathway branches correspond to three different spontaneous curvatures: positive (upper), zero (middle), and negative (lower). Pathway bifurcations occur due to different volume reduction rates imposed: slow (dotted arrow), fast (dashed arrow), or independent of the volume reduction rate (solid arrow). Only halves are shown for some vesicles for better visual effects.

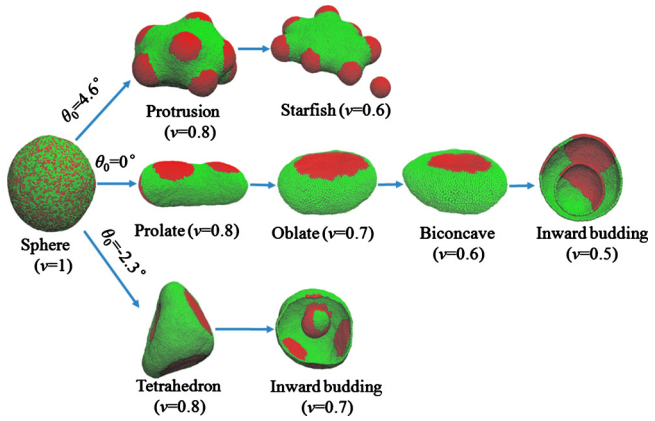

FIG. 2. (Color online) Shape transformation pathways of binary vesicles with a high compositional ratio (B:A=1:2). Three branches correspond to three different spontaneous curvatures: positive (upper), zero (middle), and negative (lower). The volume change rate dependence is not observed.

equilibrated configurations at specified reduced volume $v = V/V_{\text{sphere}}$, where V_{sphere} is the volume of the spherical vesicle. The shape transformation pathways indicated by dashed (dotted) arrows are obtained at a high (low) volume reduction rate, while those by solid arrows are independent of the volume reduction rate. The shape transformation pathways do not deviate appreciably from those of homogeneous vesicles.[26] Two overall trends are observed. First, the reduced volume effectively modulates the vesicle overall morphology, which appears to select the domain size (inversely proportional to the number of the domains). Second, the formed domains are localized in regions that match their own spontaneous curvatures to minimize the total membrane bending energy. At zero spontaneous curvature, reducing the vesicle volume first causes sphere-prolate-dumbbell transitions and then leads to pathway branching. A low volume reduction rate of $1.94\times10^{-4}\tau^{-1}$ drives dumbbell-to-tubule transition, while a high volume reduction rate of $1.75\times10^{-3}\tau^{-1}$ induces dumbbell-biconcave-inward budding transitions. The domains in this case tend to localize at relatively flat regions. At a positive spontaneous curvature ($\theta_0=4.6°$), the spherical vesicle is first transformed into the prolate shape at $v=0.8$. Further decreasing v induces prolate-tubule transition at the low volume reduction rate, but prolate-starfish transition at the high volume reduction rate. The domains in this case are localized at high-curvature regions (two ends of the prolate shape and tubule, or rims of the starfish shape), forming protrusions. At a negative spontaneous curvature ($\theta_0=-2.3°$), the vesicle features sphere-biconcave-inward budding transitions. The domains are localized at the concave regions of the biconcave shape. In the budded configurations, the domains in the outer vesicle remain in the concave regions, while those in the inner vesicle conform to the spherical shape.

At a high compositional ratio, the shape transformation pathways of binary vesicles are appreciably different, as shown in Fig. 2 (B:A=1:2). However, the domain localization mechanism remains the same. At zero spontaneous curvature, the vesicle undergoes sphere-prolate-oblate-biconcave-inward budding transitions. At a positive spontaneous curvature ($\theta_0=4.6°$), phase separation forms a shape with protrusions. Further reducing the volume causes protrusion-to-starfish transition, where a cap buds off from the mother vesicle. All the caps are now localized at the rim of the starfish. Domains with a negative spontaneous curvature ($\theta_0=-2.3°$) tend to dimple inward, inducing high curvature to the vesicle and forming a tetrahedron-like shape at $v=0.8$. Further reducing the volume to $v=0.7$ causes inward budding. Interestingly, the shape transformation pathways at the high compositional ratio are independent of the volume reduction rate. The volume reduction rate and the in-plane diffusion of the membrane particles set two time scales and play the roles of membrane stress generation and relaxation, respectively.[26] At the high volume reduction rate, membrane stress induced by the volume reduction may not be fully relaxed by particle diffusion in a short time, which alters the shape transformation pathways. However, at high compositional ratio, the line tension of the formed domains seems to dominate the membrane stress, and thus the shape transformation is nearly independent of the volume reduction rate.

The formed domains interact with each other through their elastic fields and are thus kinetically trapped due to the significant energy barrier, against further coarsening.[32,33] To better understand the dynamic coupling between vesicle shape transformation and domain growth, we next present the dynamic evolution of the vesicles. The values for the model parameters, μ, ϵ, and ς, remain unchanged. The simulations started from specific shapes instead of spherical vesicles with the compositional ratio of 1:2. Throughout the simulations, the vesicle remains at the specified reduced volumes. Figures 3(a) and 3(b) depict the dynamic domain growth and the shape transformation starting from a biconcave vesicle. At zero spontaneous curvature (a), randomly distributed particles undergo phase separation and are coarsened into small domains, which further coalesce into bigger domains. The small domains diffuse to the centers of the top and bottom surfaces and finally merge into two large ones with one on each side. The vesicle shape during domain coarsening is hardly changed. In contrast, at a positive spontaneous curvature of the secondary phase ($\theta_0=2.3°$), domain coarsening causes biconcave-starfish transition. In the end, all the domains are localized at the rim of the starfish. Figures 3(c) and 3(d) depict the dynamic domain growth and vesicle shape transformation starting from the tubule shape.

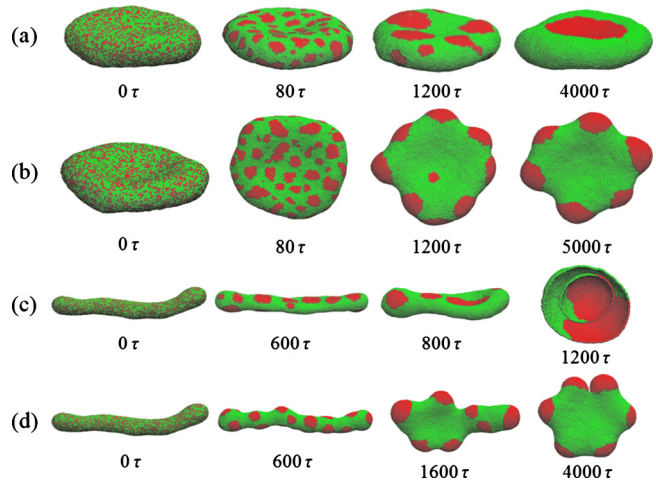

FIG. 3. (Color online) Domain growth dynamics coupled with vesicle morphogenesis. (a) $v=0.6$, $\theta_0=0°$; (b) $v=0.5$, $\theta_0=2.3°$; (c) $v=0.45$, $\theta_0=0°$; and (d) $v=0.45$, $\theta_0=2.3°$.

At zero spontaneous curvature of the secondary phase, phase separation and domain interactions lead to tubule-inward budding transition, while at a positive spontaneous curvature ($\theta_0=2.3°$), tubule-starfish transition occurs. Such drastic shape transformations are clearly aided by the domain coarsening.

In summary, through systematic particle dynamics simulations, we demonstrated the intimate coupling between the compositional ratio, spatial domain organization, and vesicle shape transformation. Our simulations showed that the overall vesicle shape may direct the spatial organization of the membrane domains, which indicates a sorting mechanism of membrane domains based on their material properties. Reciprocally, membrane domains may lead to long-range remodeling of vesicles, an important step toward cellular transport. We also showed that volume reduction rate affects the shape transformation pathways only at relatively low compositional ratio. Our simulation results suggest the essential role of membrane domains in protein and lipid sorting.

This work was supported by the National Science Foundation under Grant No. CMMI-0826841.

[1]D. A. Brown and E. London, Annu. Rev. Cell Dev. Biol. **14**, 111 (1998).
[2]D. C. Hoessli, S. Ilangumaran, A. Soltermann, P. J. Robinson, B. Borisch, and N. U. Din, Glycoconjugate J. **17**, 191 (2000).
[3]L. J. Pike, J. Lipid Res. **44**, 655 (2003).
[4]M. Edidin, Annu. Rev. Biophys. Biomol. Struct. **32**, 257 (2003).
[5]C. Salaun, D. J. James, and L. H. Chamberlain, Traffic (Oxford, U. K.) **5**, 255 (2004).
[6]S. L. Zhang, J. Li, G. Lykotrafitis, G. Bao, and S. Suresh, Adv. Mater. (Weinheim, Ger.) **21**, 419 (2009).
[7]H. Y. Yuan and S. L. Zhang, Appl. Phys. Lett. **96**, 033704 (2010).
[8]K. Hanada, K. Kumagai, S. Yasuda, Y. Miura, M. Kawano, M. Fukasawa, and M. Nishijima, Nature (London) **426**, 803 (2003).
[9]B. J. Peter, H. M. Kent, I. G. Mills, Y. Vallis, P. J. G. Butler, P. R. Evans, and H. T. McMahon, Science **303**, 495 (2004).
[10]H. T. McMahon and J. L. Gallop, Nature (London) **438**, 590 (2005).
[11]A. Frost, R. Perera, A. Roux, K. Spasov, O. Destaing, E. H. Egelman, P. De Camilli, and V. M. Unger, Cell **132**, 807 (2008).
[12]R. Phillips, T. Ursell, P. Wiggins, and P. Sens, Nature (London) **459**, 379 (2009).
[13]A. Roux, D. Cuvelier, P. Nassoy, J. Prost, P. Bassereau, and B. Goud, EMBO J. **24**, 1537 (2005).
[14]R. Parthasarathy, C. H. Yu, and J. T. Groves, Langmuir **22**, 5095 (2006).
[15]H. Y. Jiang and T. R. Powers, Phys. Rev. Lett. **101**, 018103 (2008).
[16]M. Heinrich, A. Tian, C. Esposito, and T. Baumgart, Proc. Natl. Acad. Sci. U.S.A. **107**, 7208 (2010).
[17]H. J. Risselada and S. J. Marrink, Proc. Natl. Acad. Sci. U.S.A. **105**, 17367 (2008).
[18]T. S. Ursell, W. S. Klug, and R. Phillips, Proc. Natl. Acad. Sci. U.S.A. **106**, 13301 (2009).
[19]H. Y. Yuan, C. J. Huang, J. Li, G. Lykotrafitis, and S. L. Zhang, Phys. Rev. E **82**, 011905 (2010).
[20]P. B. Sunil Kumar, G. Gompper, and R. Lipowsky, Phys. Rev. Lett. **86**, 3911 (2001).
[21]M. Laradji and P. B. Sunil Kumar, Phys. Rev. Lett. **93**, 198105 (2004).
[22]G. Brannigan, P. F. Philips, and F. L. H. Brown, Phys. Rev. E **72**, 011915 (2005).
[23]I. R. Cooke, K. Kremer, and M. Deserno, Phys. Rev. E **72**, 011506 (2005).
[24]A. P. Lyubartsev, Eur. Biophys. J. **35**, 53 (2005).
[25]S. J. Marrink, H. J. Risselada, S. Yefimov, D. P. Tieleman, and A. H. de Vries, J. Phys. Chem. B **111**, 7812 (2007).
[26]H. Y. Yuan, C. J. Huang, and S. L. Zhang, Soft Matter **6**, 4571 (2010).
[27]C. Dietrich, L. A. Bagatolli, Z. N. Volovyk, N. L. Thompson, M. Levi, K. Jacobson, and E. Gratton, Biophys. J. **80**, 1417 (2001).
[28]C. Zheng, P. Liu, J. Li, and Y.-W. Zhang, Langmuir **26**, 12659 (2010).
[29]G. Lykotrafitis, S. Zhang, H. Li, and J. Li (unpublished).
[30]T. Baumgart, S. Das, W. W. Webb, and J. T. Jenkins, Biophys. J. **89**, 1067 (2005).
[31]T. Baumgart, S. T. Hess, and W. W. Webb, Nature (London) **425**, 821 (2003).
[32]T. R. Weikl, M. M. Kozlov, and W. Helfrich, Phys. Rev. E **57**, 6988 (1998).
[33]M. Yanagisawa, M. Imai, and T. Taniguchi, Phys. Rev. Lett. **100**, 148102 (2008).